# Photocatalytic Overall Water Splitting under Visible Light Using $ATaO_2N$ (A = Ca, Sr, Ba) and $WO_3$ in a $IO_3^-/I^-$ Shuttle Redox Mediated System

Masanobu Higashi,[†] Ryu Abe,*[,‡] Tsuyoshi Takata,[†] and Kazunari Domen[†]

*Faculty of Engineering, The University of Tokyo, 7-3-1 Hongo, Bunkyo-ku, Tokyo, 113-8656, Japan, and Catalysis Research Center, Hokkaido University, Sapporo 001-0021, Japan*

*Received November 19, 2008. Revised Manuscript Received February 24, 2009*

Three mixed tantalum oxynitrides, $ATaO_2N$ (A = Ca, Sr, Ba), prepared by heating amorphous $A_2Ta_2O_7$ under $NH_3$, are applied in a two-step photoexcitation water-splitting system as a photocatalyst for $H_2$ evolution. Platinum-loaded $CaTaO_2N$ and $BaTaO_2N$ are demonstrated to be active for $H_2$ evolution in the presence of methanol or $I^-$ as an electron donor, whereas $SrTaO_2N$ is unable to produce $H_2$ stably in the presence of $I^-$ due to self-oxidative decomposition accompanied by $N_2$ production. The combination of Pt−$CaTaO_2N$ or Pt−$BaTaO_2N$ with Pt−$WO_3$ achieves overall water splitting under visible irradiation. Pt−$BaTaO_2N$ is also demonstrated to be photoactive at wavelengths up to 660 nm, representing the first example of an overall water-splitting system in which visible light at wavelengths longer than 600 nm is effectively utilized for $H_2$ evolution.

## Introduction

Photocatalytic water splitting into $H_2$ and $O_2$ using a semiconductor catalyst has received much attention recently due to the potential of this method for the clean production of $H_2$ from water utilizing solar energy. Although a number of metal oxides[1−17] have been reported to be active photocatalysts for the water-splitting reaction, most only function under ultraviolet (UV) light ($\lambda < 400$ nm) owing to the large band gap energy of the materials (>3 eV). Because almost half of all incident solar energy at the Earth's surface falls in the visible region ($400 < \lambda < 800$ nm), the efficient utilization of visible light remains indispensable for realizing practical $H_2$ production based on photocatalytic water splitting. The present authors have recently demonstrated photocatalytic overall water splitting under visible light ($\lambda < 500$ nm) by two different approaches.[18−23] The focus of research has subsequently turned to achieving more efficient utilization of visible light by widening the band of photoabsorption and increasing the quantum efficiency of the photocatalyst. A two-step water-splitting system[20−24] utilizing a reversible redox couple, such as iodate/iodide ($IO_3^-/I^-$) and $Fe^{3+}/Fe^{2+}$, is possibly the most promising means of extending the available wavelength region. In such a system, the photon energy required to drive each photocatalyst is smaller than that required in the one-step process. However, only a limited part of the visible spectrum ($\lambda < 500$ nm) has been utilized to date, due primarily to difficulty in developing visible light-responsive photocatalysts for $H_2$ production.

The oxide semiconductors have two key properties: the valence bands are comprised of O 2p orbitals and the bands are fixed at deeply positive levels.[25] The present authors have recently reported several stable oxynitride photocatalysts[26−30]

* To whom correspondence should be addressed.
[†] The University of Tokyo.
[‡] Hokkaido University.

(1) Domen, K.; Naito, S.; Soma, M.; Tamaru, T. *J. Chem. Soc., Chem. Commun.* **1980**, 543.
(2) Lehn, J.; Sauvage, J.; Ziessel, R.; Halaire, L *Isr. J. Chem.* **1982**, *22*, 168.
(3) Domen, K.; Kudo, A.; Ohnishi, T. *J. Catal.* **1986**, *102*, 92.
(4) Kato, H.; Kudo, A. *Chem. Phys. Lett.* **1998**, *295*, 487.
(5) Kato, H.; Kudo, A. *Chem. Phys. Lett.* **2000**, *331*, 373.
(6) Kato, H.; Asakura, K.; Kudo, A. *J. Am. Chem. Soc.* **2003**, *125*, 3082.
(7) Kato, H.; Kudo, A. *Catal. Today* **2003**, *78*, 561.
(8) Domen, K.; Kudo, A.; Shinozaki, A.; Tanaka, A.; Maruya, K.; Onisihi, T. *J. Chem. Soc., Chem. Commun.* **1986**, 356.
(9) Kudo, A.; Tanaka, A.; Domen, K.; Maruya, K.; Aika, K.; Onishi, T. *J. Catal.* **1988**, *111*, 67.
(10) Abe, R.; Higashi, M.; Zou, Z.; Sayama, K.; Abe, Y.; Arakawa, H. *Chem. Lett.* **2004**, *33*, 954.
(11) Shimizu, K.; Tsuji, Y.; Kawakami, M.; Toda, K.; Kodama, T.; Sato, M.; Kitayama, Y. *Chem. Lett.* **2002**, *31*, 1158.
(12) Shimizu, K.; Itoh, S.; Hatamachi, T.; Kodama, T.; Sato, M.; Toda, K. *Chem. Mater.* **2005**, *17*, 5161.
(13) Machida, M.; Mitsuyama, T.; Ikeue, K. *J. Phys. Chem. B* **2005**, *109*, 7801.
(14) Miseki, Y.; Kato, H.; Kudo, A. *Chem. Lett.* **2006**, *35*, 9.
(15) Sato, J.; Saito, N.; Nishimiya, H.; Inoue, Y. *J. Phys. Chem. B* **2001**, *105*, 6061.
(16) Ikarashi, K.; Sato, J.; Kobayashi, H.; Saito, N.; Inoue, Y. *J. Phys. Chem. B* **2002**, *106*, 9048.
(17) Sato, J.; Kobayashi, H.; Ikarashi, K.; Saito, N.; Nishimiya, H.; Inoue, Y. *J. Phys. Chem. B* **2004**, *108*, 4369.
(18) Maeda, K.; Teramura, K.; Lu, D.; Takata, T.; Saito, N.; Inoue, Y.; Domen, K. *Nature* **2006**, *440*, 295.
(19) Lee, Y.; Terashima, H.; Shimodaira, Y.; Teramura, K.; Hara, M.; Kobayashi, H.; Domen, K.; Yashima, M. *J. Phys. Chem. C* **2007**, *111*, 1042.
(20) Abe, R.; Takata, T.; Sugihara, H.; Domen, K. *Chem. Commun.* **2005**, 3829.
(21) Abe, R.; Sayama, K.; Domen, K.; Arakawa, H. *Chem. Phys. Lett.* **2001**, *344*, 339.
(22) Sayama, K.; Mukasa, K.; Abe, R.; Abe, Y.; Arakawa, H. *Chem. Commun.* **2001**, 2416.
(23) Abe, R.; Sayama, K.; Sugihara, H. *J. Phys. Chem. B* **2005**, *109*, 16052.
(24) Kato, H.; Hori, M.; Konta, R.; Shimodaira, Y.; Kudo, A. *Chem. Lett.* **2004**, *33*, 1348.
(25) Sacaife, D. E. *Sol. Energy* **1980**, *25*, 41.
(26) Kasahara, A.; Nukumizu, K.; Hitoki, G.; Takata, T.; Kondo, J. N.; Hara, M.; Kobayashi, H.; Domen, K. *J. Phys. Chem. A* **2002**, *106*, 6750.

10.1021/cm803145n CCC: $40.75 
Published on Web 03/26/2009

as potential candidates for visible light-induced water splitting. It has been confirmed that the valence bands of these oxynitride materials are populated by N 2p and O 2p orbitals, resulting in more negative valence band levels and smaller band gaps compared to conventional oxide semiconductors, allowing visible light-induced $H_2$ production from water. Steady overall water splitting has been demonstrated in an $IO_3^-/I^-$ shuttle redox mediated system using a simple tantalum oxynitride (TaON) loaded with platinum as an $H_2$ evolution photocatalyst in combination with $Pt-WO_3$ or $RuO_2-TaON$.[20,31] However, the system is photoactive only to wavelengths shorter than 500 nm, leaving much of the visible spectrum unutilized.

In the present study, three mixed tantalum oxynitrides, $ATaO_2N$ (A = Ca, Sr, Ba), with absorption edges at longer wavelengths than for TaON, are prepared and applied in a two-step photoexcitation water-splitting system as an $H_2$ evolution photocatalyst. $CaTaO_2N$ and $BaTaO_2N$ are found to display activity for $H_2$ evolution in the presence of methanol or $I^-$ as an electron donor, and in combination with $Pt-WO_3$ realize an effective system for overall water splitting under visible light. $Pt-BaTaO_2N$ is also demonstrated to be photoactive for $H_2$ evolution at wavelengths up to 660 nm.

## Experimental Section

**Materials.** Powders of the $A_2Ta_2O_7$ precursors were prepared by a polymerized complex (PC) method,[32,33] as follows. Methanol (ca. 50 mL) was used as a solvent to dissolve 0.02 mol of $TaCl_5$. A large excess of citric acid (CA, ca. 0.3 mol) was added into the methanol solution of $TaCl_5$ with continuous stirring to produce metal−CA complexes. After complete dissolution of the CA, 0.02 mol of $ACO_3$ (A = Ca, Sr, Ba) was added to the solution. The mixture was then magnetically stirred for 1 h to afford a transparent solution of the metal−CA complexes. Subsequently, 1.2 mol of ethylene glycol (EG) was added to this solution, and the clear mixture thus obtained was heated at 303 K to remove the methanol and accelerate esterification reactions between CA and EG. Upon continuous heating at ca. 303 K, the solution became highly viscous and changed in color from colorless to deep brown, eventually gelling into a glassy transparent-brown resin. The resin was charred in a mantle heater for 1 h at ca. 623 K to afford a black solid mass, which was finally calcined on an $Al_2O_3$ plate at 873 K in ambient air.

Powders of oxynitride $ATaO_2N$ were prepared by heating the precursor (ca. 1 g) under $NH_3$ flow (100 mL $min^{-1}$) at 1123−1273 K for 20 h. $WO_3$ powder (99.99%) was provided by Kojundo Chemical Laboratory Co., Ltd., Japan. All other chemicals used in the experiments were purchased from commercial sources as guaranteed reagents and used without further purification.

**Characterization of Catalysts.** The prepared samples were studied by powder X-ray diffraction (XRD; RINT2500HR-PC, Rigaku; Cu Kα), scanning electron microscopy (SEM; S-4700, Hitachi), and UV−visible diffuse reflectance spectroscopy (DRS; V-560, Jasco). The Brunauer, Emmett, Teller (BET) surface area was measured using a Coulter SA-3100 instrument at liquid nitrogen temperature.

**Photocatalytic Reactions.** The $ATaO_2N$ was loaded with 0.3 wt % platinum by impregnation from an aqueous $H_2PtCl_6$ solution followed by $H_2$ reduction for 1 h at 473 K. In the case of $WO_3$, 0.5 wt % platinum was loaded by impregnation from an aqueous $H_2PtCl_6$ solution followed by calcination at 623 K in air for 30 min. Photocatalytic reactions were carried out in a Pyrex reaction vessel connected to a closed gas circulation system. $H_2$ evolution was examined using 250 mL aqueous solutions containing 0.1 g of $Pt-ATaO_2N$ and 50 mL of methanol (20 vol %) or 1.25 mmol of NaI as an electron donor. In the case of two-step water-splitting reactions, the $Pt-ATaO_2N$ and $Pt-WO_3$ photocatalysts (0.1 g of each) were suspended in 5 mM NaI aqueous solution. The reaction solution was then thoroughly degassed, and then exposed to 5 kPa of argon. The reaction solution was irradiated using a xenon lamp (300 W) fitted with a cutoff filter and water filters to eliminate light in the UV and infrared regions, respectively. The evolved gases were analyzed by online gas chromatography, and the amounts of $I_3^-$ and $IO_3^-$ anions produced by the reactions were determined by UV−visible absorption spectroscopy and ion chromatography, respectively.

## Results and Discussion

**Characterizations of Materials.** Figure 1 shows the XRD patterns of $ATaO_2N$ (A = Ca, Sr, Ba) samples prepared by heating amorphous $A_2Ta_2O_7$ precursors at various temperatures for 20 h under $NH_3$ flow (100 mL $min^{-1}$). In the XRD patterns of $CaTaO_2N$ and $SrTaO_2N$ samples prepared at temperatures above 1123 K, only the peaks corresponding to the perovskite phase were observed, in good agreement with previous reports.[34,35] No peaks assignable to the respective oxide forms (e.g., $Ca_2Ta_2O_7$ or $Sr_2Ta_2O_7$) were observed. In addition to the main peaks derived from the perovskite phase, weak peaks assignable to the $Ta_3N_5$ phase were clearly observable for $BaTaO_2N$ at all heating temperatures (Figure 1c). Even with careful control of the preparation conditions, the formation of the $Ta_3N_5$ phase could not be prevented for $BaTaO_2N$ samples in the present study. With increasing ionic radius of $A^{2+}$, from $Ca^{2+}$ (1.34 Å) to $Ba^{2+}$ (1.61 Å), the intensity of the peak at $2\theta \approx 23°$ decreased, indicating an increase in the symmetry of the perovskite structure, as reported previously.[35]

Figure 2 shows SEM images of the prepared $ATaO_2N$ samples. $CaTaO_2N$ and $SrTaO_2N$ exhibit distinct crystal growths for samples prepared at 1123−1273 K, in agreement with the increasing intensity of the XRD peaks (Figure 1). These samples generally appear as highly aggregated forms with constituent particles of less than 100 nm in diameter. In contrast, all of the $BaTaO_2N$ samples consist of particles of 100−200 nm in size. The size of the particles increased with temperature above 1173 K.

(27) Kasahara, A.; Nukumizu, K.; Takata, T.; Kondo, J. N.; Hara, M.; Kobayashi, H.; Domen, K. *J. Phys. Chem. B* **2003**, *107*, 791.
(28) Hitoki, G.; Takata, T.; Kondo, J. N.; Hara, M.; Kobayashi, H.; Domen, K. *Chem. Commun.* **2002**, 1698.
(29) Hara, M.; Hitoki, G.; Takata, T.; Kondo, J. N.; Kobayashi, H.; Domen, K. *Catal. Today* **2003**, *78*, 555.
(30) Hitoki, G.; Ishikawa, A.; Takata, T.; Kondo, J. N.; Hara, M.; Domen, K. *Chem. Lett.* **2002**, 736.
(31) Kakihana, M.; Milanova, M. M.; Arima, M.; Okubo, T.; Yashima, M.; Yoshimura, M. *J. Am. Ceram. Soc.* **1996**, *79*, 1673.
(32) Yoshimoto, M.; Kakihana, M.; Cho, W.; Kato, H.; Kudo, A. *Chem. Mater.* **2002**, *14*, 3369.
(33) Marchand, R.; Pors, F.; Laurent, Y. *Rev. Int. Hautes Temp. Refract.* **1986**, *23*, 11.
(34) Günther, E.; Hagenmayer, R.; Jansen, M. *Z. Anorg. Allg. Chem.* **2000**, *626*, 1519.
(35) Kim, Y.; Woodward, P. M.; Baba-Kishi, K. Z.; Tai, C. W. *Chem. Mater.* **2004**, *16*, 1267.

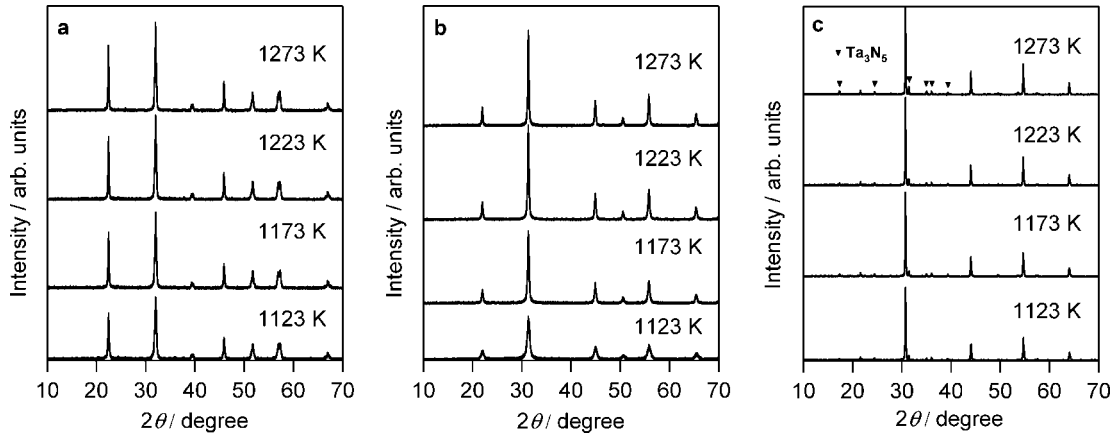


**Figure 1.** XRD patterns of (a) $CaTaO_2N$, (b) $SrTaO_2N$, and (c) $BaTaO_2N$ samples obtained by nitriding amorphous $A_2Ta_2O_7$ at 1123−1273 K for 20 h under $NH_3$ flow.

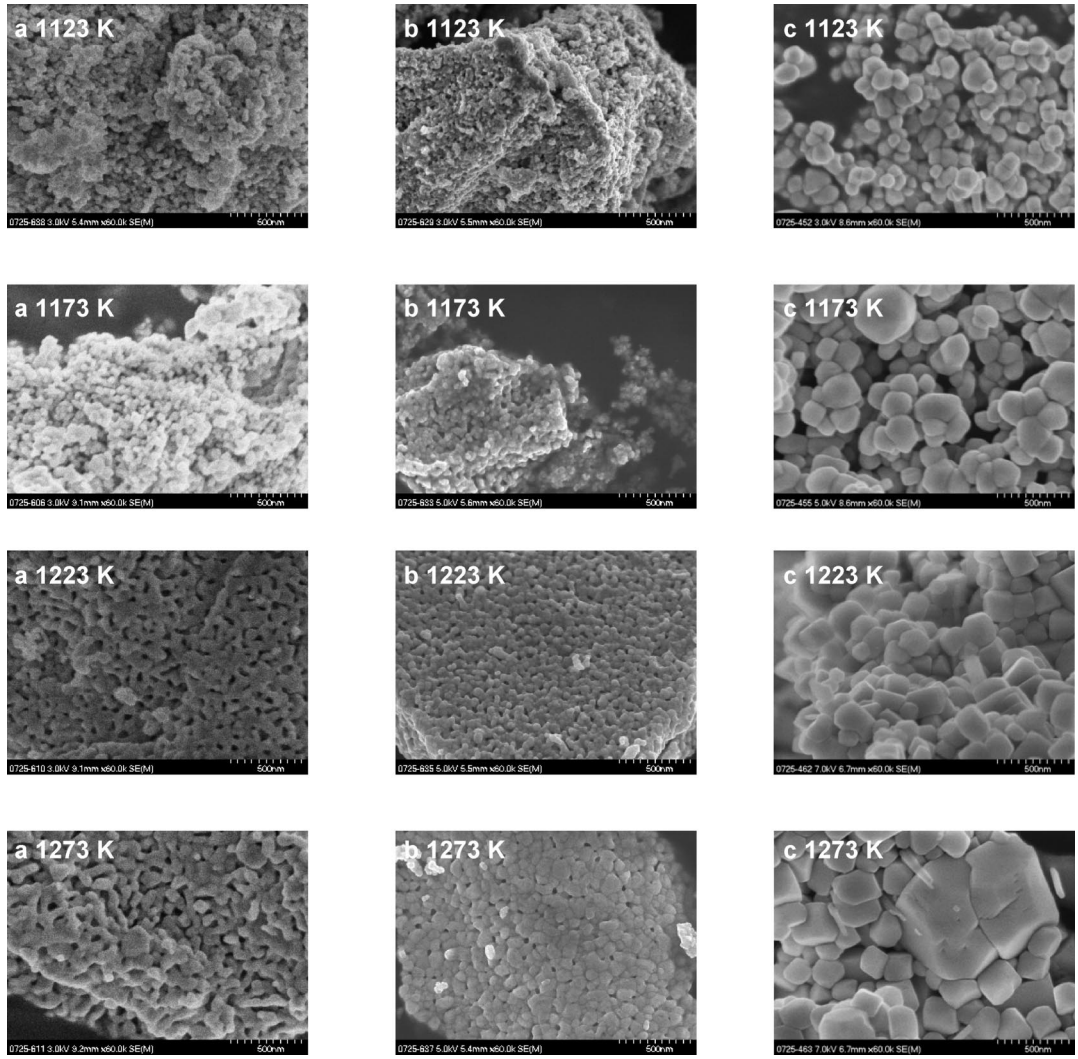


**Figure 2.** SEM images of (a) $CaTaO_2N$, (b) $SrTaO_2N$, and (c) $BaTaO_2N$ samples obtained by nitriding amorphous $A_2Ta_2O_7$ at 1123−1273 K for 20 h under $NH_3$ flow.

Figure 3 shows the UV−vis diffuse reflectance spectra for the $ATaO_2N$ samples. The absorption spectra for $CaTaO_2N$ and $SrTaO_2N$ are invariant with respect to heating temperature in the range from 1173 to 1223 K, and the samples prepared at 1123 K exhibited only minor differences. The spectra for the $BaTaO_2N$ samples, however, display substantial changes with increasing temperature. The $BaTaO_2N$ samples prepared at low temperatures (1123 and 1173 K) exhibit a monotonically increasing absorption at wavelengths longer than 700 nm. Such photoabsorption is known to be attributable to the presence of anion vacancies or reduced metal cation species in the semiconductor, where

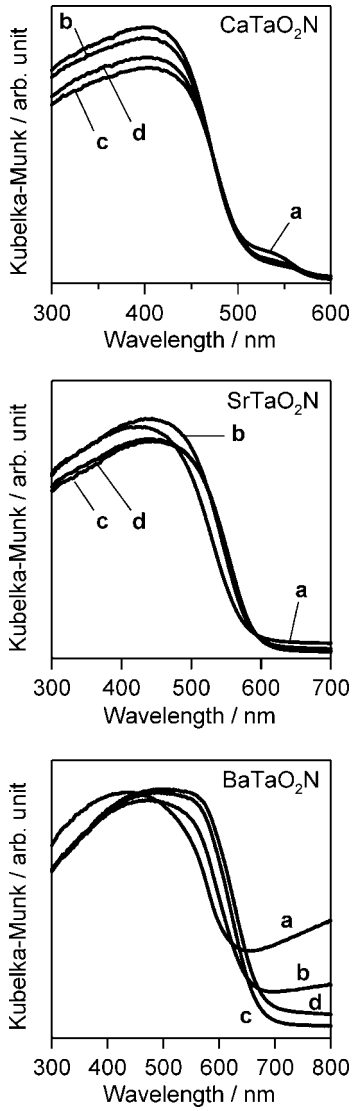


**Figure 3.** Diffuse reflectance spectra for $CaTaO_2N$, $SrTaO_2N$, and $BaTaO_2N$ samples obtained by nitriding amorphous $A_2Ta_2O_7$ at (a) 1123, (b) 1173, (c) 1223, and (d) 1273 K for 20 h under $NH_3$ flow.

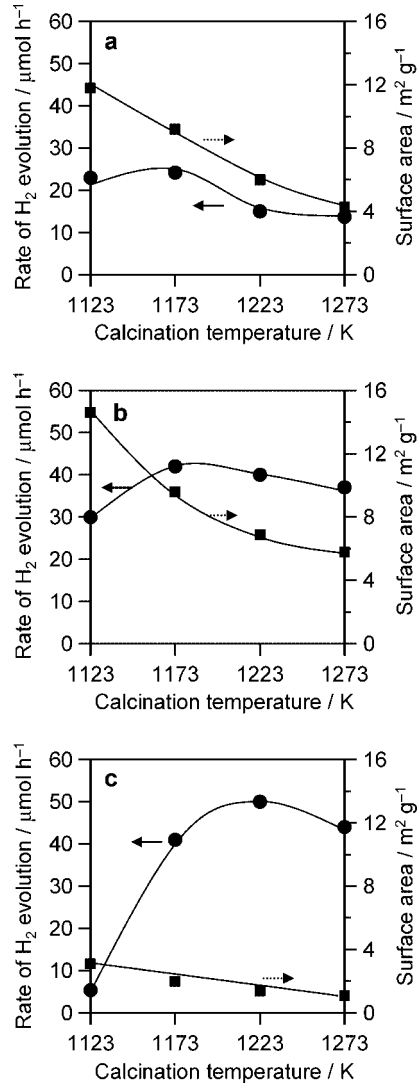


**Figure 4.** Preparation temperature dependence of photocatalytic activity of (a) Pt−$CaTaO_2N$, (b) Pt−$SrTaO_2N$, and (c) Pt−$BaTaO_2N$ for $H_2$ evolution from aqueous methanol solution under visible light ($\lambda > 420$ nm).

the available electron can readily be excited to empty conduction band levels by absorbing light at even low energies. The absorption exhibited by the $BaTaO_2N$ samples at longer wavelengths ($\lambda > 660$ nm) is thus considered to reflect the presence of anion vacancies or reduced $Ta^{5+}$ species (e.g., $Ta^{4+}$) in the samples prepared at low temperatures. The absorbance at longer wavelength decreased with increasing heating temperature, and the $BaTaO_2N$ samples prepared at above 1223 K display a distinct absorption edge at ca. 660 nm. The absorption edges of $ATaO_2N$ determined from these spectra are 520 (Ca), 600 (Sr), and 660 nm (Ba), corresponding to a shift to longer wavelength with increasing ionic radius of $A^{2+}$ ($Ca^{2+}$, 1.34 Å; $Sr^{2+}$, 1.44 Å; $Ba^{2+}$, 1.61 Å).

These results indicate that a series of mixed oxynitrides, $ATaO_2N$ (A = Ca, Sr, Ba), with perovskite structures can be obtained by $NH_3$ treatment of amorphous $A_2Ta_2O_7$ precursors. The two main issues encountered in the present preparations, that is, the formation of an impurity $Ta_3N_5$ phase in the synthesis of $BaTaO_2N$, and the generation of anion vacancies or reduced tantalum species at low temperature, appear to be attributable to inhomogeneities in the occurrence of barium and tantalum species in the amorphous precursors prepared by the PC technique. Such inhomogeneities can be expected to result in phase separation between tantalum- and barium-rich phases during heat treatment of the precursor under $NH_3$. The tantalum-rich species would then be responsible for the formation of the $Ta_3N_5$ impurity phase, whereas the generation of reduced tantalum species would be associated with the barium-rich species. Such problems in $BaTaO_2N$ preparation were not reported in the preparation of $BaTaO_2N$ by direct ammonolysis using a powder mixture of $BaCO_3$ and $Ta_2O_5$.[34,35]

**$H_2$ Evolution from Aqueous Methanol Solution.** All of the platinum-loaded $ATaO_2N$ samples were confirmed to exhibit photocatalytic activity for $H_2$ evolution from water under visible light in the presence of methanol as a sacrificial electron donor, without detectable $N_2$ evolution due to self-oxidative decomposition. The rates of $H_2$ evolution over the Pt−$ATaO_2N$ samples are plotted as a function of preparation temperature in Figure 4. The specific surface areas for each sample are also shown. The rate of $H_2$ evolution over

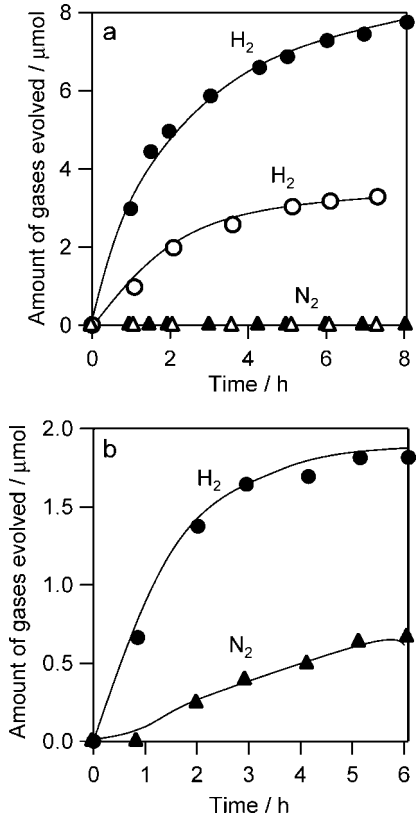


**Figure 5.** Time courses of $H_2$ evolution over (a) Pt−$CaTaO_2N$ (solid marks), Pt−$BaTaO_2N$ (open marks), and (b) Pt−$SrTaO_2N$ (0.1 g) under visible light ($\lambda > 420$ nm) in the presence of 5 mM NaI.

Pt−$CaTaO_2N$ and Pt−$SrTaO_2N$ increased slightly with heating temperature from 1123 to 1173 K, attributable to the increase in crystallinity as indicated by the XRD and SEM results. The rate of evolution decreased slightly for the higher temperature samples, possibly due to the decrease in specific surface area. The rate of $H_2$ evolution over Pt−$BaTaO_2N$ increased markedly with preparation temperature from 1123 to 1223 K (Figure 4c). As described above, the $BaTaO_2N$ samples are likely to host anion vacancies and reduced metal species such as $Ta^{4+}$. Such anion vacancies or reduced species are known to act as recombination centers for photogenerated carriers (i.e., electrons and holes). The presence of elevated densities of such sites can therefore be expected to degrade the photocatalytic activity of the semiconductor material. The increase in activity with preparation temperature reflects the decrease in the density of anion vacancies and reduced species in $BaTaO_2N$ as the preparation temperature increases from 1123 to 1223 K. Such an effect would be in addition to the increase in crystallinity. The optimum preparation temperatures for achieving the highest $H_2$ evolution rate are 1173 K for $CaTaO_2N$ and $SrTaO_2N$ and 1223 K for $BaTaO_2N$, and the optimized $H_2$ evolution rate decreases in the order $BaTaO_2N$ (50 $\mu$mol $h^{-1}$) > $SrTaO_2N$ (42 $\mu$mol $h^{-1}$) > $CaTaO_2N$ (24 $\mu$mol $h^{-1}$).

**$H_2$ Evolution from Aqueous NaI Solution.** The present oxynitrides were also tested as photocatalysts for $H_2$ evolution from water in the presence of $I^-$ as an electron donor. The reactions were carried out in slightly acidic (pH ~6) solutions, which were obtained by the addition of solute (NaI) and photocatalyst powders into pure water. Figure 5a shows the time courses of $H_2$ evolution over Pt−$BaTaO_2N$ and Pt−$CaTaO_2N$ from an aqueous solution of NaI (5 mM) under visible irradiation ($\lambda > 420$ nm). The rate of $H_2$ evolution gradually decreased during prolonged irradiation and eventually ceased in both cases. The production of $IO_3^-$ anions in the solution was also confirmed, although accurate quantitative determination of $IO_3^-$ was difficult due to low concentrations and the adsorption of $IO_3^-$ onto the photocatalyst powder. No $H_2$ evolution was observed in the absence of $I^-$ in the solution. The following reactions are thus considered to occur on the Pt−$BaTaO_2N$ and Pt−$CaTaO_2N$ photocatalyst under visible light:

$$BaTaO_2N \text{ (or } CaTaO_2N) + h\nu\ (\lambda > 420 \text{ nm}) \rightarrow e^- + h^+ \quad (1)$$

$$2H^+ + 2e^- \rightarrow H_2 \quad (2)$$

$$I^- + 3H_2O + 6h^+ \rightarrow IO_3^- + 6H^+ \quad (3)$$

The cessation of $H_2$ production observed during prolonged irradiation can be explained by the backward reaction taking place over the reduction site (Pt) of the photocatalyst. That is, the preferential reduction of $IO_3^-$ anion to $I^-$ occurs instead of water reduction:[20−22]

$$IO_3^- + 6H^+ + 6e^- \rightarrow I^- + 3H_2O \quad (4)$$

As shown in Figure 5a, the amount of $H_2$ produced on Pt−$CaTaO_2N$ was larger than that on Pt−$BaTaO_2N$, suggesting that the backward reaction (eq 4) is also dependent on the photocatalyst material itself, not just on the Pt cocatalyst. No $N_2$ evolution was observed during the reaction in either case.

It has been reported that some (oxy)nitrides suffer from self-oxidative decomposition,[26,27] whereby nitrogen anions ($N^{3-}$) are oxidized to $N_2$ by photogenerated holes:

$$2N^{3-} + 6h^+ \rightarrow N_2 \quad (5)$$

A considerable amount of $N_2$ was evolved over Pt−$SrTaO_2N$ accompanying $H_2$ evolution under visible irradiation in the solution containing NaI (Figure 5b). This can be explained by the self-oxidative decomposition of the $SrTaO_2N$ material as described by eq 5. At present, the reason for the greater instability of $SrTaO_2N$ compared to that of the other $ATaO_2N$ samples is unclear. However, judging from the stable production of $H_2$ over Pt−$SrTaO_2N$ from aqueous methanol solution without $N_2$ generation, self-oxidative decomposition is likely to be promoted by the reaction of strontium cations with iodide ($I^-$) or iodate ($IO_3^-$).

**Two-Step Water Splitting under Visible Light.** Overall water splitting under visible light was attempted using a combination of Pt−$ATaO_2N$ and Pt−$WO_3$ as an $O_2$ evolution photocatalyst. As reported previously, the Pt−$WO_3$ photocatalyst possesses unique reactivity for the oxidation of water, realizing selective $O_2$ evolution in the presence of $IO_3^-$ electron acceptors even at low $IO_3^-$ concentrations.[22,23] Figure 6 shows the time courses of gas evolution under visible light ($\lambda > 420$ nm) using a mixture of Pt−$BaTaO_2N$ prepared at

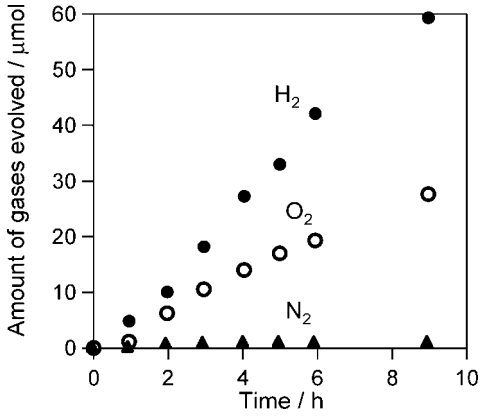


**Figure 6.** Time courses of gas evolution over a mixture of Pt−$WO_3$ and Pt−$BaTaO_2N$ under visible light ($\lambda > 420$ nm) in the presence of 5 mM NaI (Pt(0.3 wt %)−$BaTaO_2N$, 0.1 g; Pt(0.5 wt %)−$WO_3$, 0.1 g).

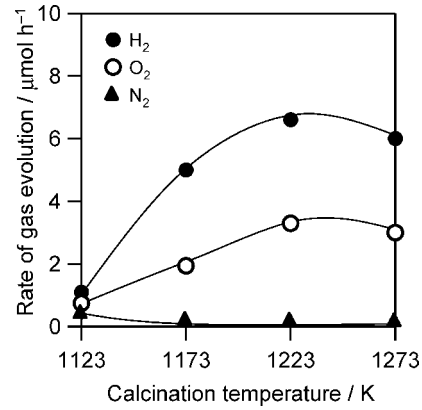


**Figure 7.** Preparation temperature dependence of photocatalytic activity of a combination of Pt−$WO_3$ and Pt−$BaTaO_2N$ under visible light ($\lambda >$ 420 nm) in an $I^-/IO_3^-$ shuttle redox mediated system.

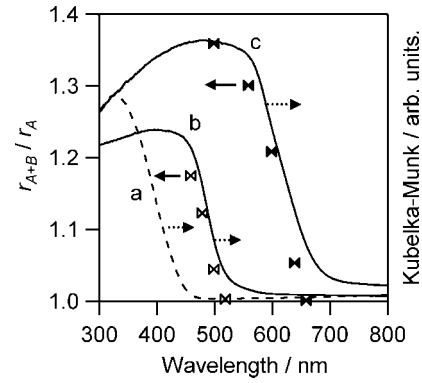


**Figure 8.** Variation in ($r_{A+B}/r_A$) ratio with cutoff wavelength of incident light (illuminator B) and absorption spectra for (a) $WO_3$, (b) $CaTaO_2N$, and (c) $BaTaO_2N$.

1223 K and Pt−$WO_3$ suspended in aqueous NaI solution (5 mM). The combination of Pt−$BaTaO_2N$ and Pt−$WO_3$ photocatalysts allows simultaneous $H_2$ and $O_2$ evolution from NaI aqueous solution under visible light at a close to stoichiometric ratio ($H_2$:$O_2$ = 2:1). A small degree of $N_2$ evolution was also observed in the first run. No gas evolution was observed in the absence of $I^-$ anions in the solution under visible light, and no reaction took place in the dark. These results indicate that overall water splitting proceeds by a two-step photoexcitation process combined with redox cycling between $IO_3^-$ and $I^-$. The first step involves water reduction to $H_2$ and $I^-$ oxidation to $IO_3^-$ over Pt−$BaTaO_2N$, and the second step involves $IO_3^-$ reduction to $I^-$ and water oxidation to $O_2$ over Pt−$WO_3$. The apparent quantum efficiency for overall water splitting for this combination is ca. 0.1% at 420−440 nm. As shown in Figure 1, $Ta_3N_5$ impurity phase existed in $BaTaO_2N$ sample. However, no detectable $H_2$ was produced by using Pt-loaded $Ta_3N_5$ photocatalyst in the presence of iodide ($I^-$) electron donor, as far as we have examined in various conditions. Therefore, we have concluded that the $BaTaO_2N$ phase, not the $Ta_3N_5$ impurity one, acts as an $H_2$ evolution photocatalyst in the overall water-splitting system with $IO_3^-/I^-$ redox cycle. The combination of Pt−$CaTaO_2N$ and Pt−$WO_3$ also achieved simultaneous evolution of $H_2$ and $O_2$ at a near-stoichiometric ratio (Figure S1). However, the combination of Pt−$SrTaO_2N$ and Pt−$WO_3$ failed to split water (Figure S1), certainly due to the self-oxidative decomposition of $SrTaO_2N$ photocatalyst as mentioned above.

Figure 7 shows dependence of gas evolution rate over Pt−$BaTaO_2N$/Pt−$WO_3$ on the preparation temperature of the $BaTaO_2N$ sample. The tendency in overall activity (i.e., rates of $H_2$ and $O_2$ evolution) are in good agreement with the trend in the $H_2$ evolution rate from methanol solution (Figure 4). This result indicates that the $H_2$ evolution process over Pt−$BaTaO_2N$ is the rate-determining step in the present system. The rate of $N_2$ production decreased with increasing preparation temperature, suggesting self-oxidative decomposition is retarded by high crystallinity. Figure S2 showed the results on Pt−$CaTaO_2N$ and Pt−$SrTaO_2N$, which were combined with Pt−$WO_3$.

**Wavelength Dependence of Activity for Overall Water Splitting.** Based on the absorption spectrum of $BaTaO_2N$, it is expected that $H_2$ evolution over Pt−$BaTaO_2N$ proceeds by the absorption of visible light at wavelengths up to 660 nm. For confirmation of this behavior, the dependence of $H_2$ evolution over Pt−$BaTaO_2N$ on the wavelength of irradiation in overall water splitting was examined using two xenon illuminators (A and B) with different emission characteristics. Illuminator A emits light at wavelengths longer than 420 nm ($4.32 \times 10^{22}$ photons·$h^{-1}$ at 420 nm $< \lambda <$ 660 nm), whereas illuminator B is fitted with a number of cutoff filters to produce only light with wavelength longer than 500 nm ($2.54 \times 10^{22}$ photons·$h^{-1}$ at 500 nm $< \lambda <$ 660 nm). Illuminator B is designed to excite $BaTaO_2N$ but not $WO_3$ (absorption edge, 450 nm). As the concentration of $IO_3^-$ in the solution was negligibly small after the overall splitting reaction (Figure 6), the $H_2$ evolution rate over Pt−$BaTaO_2N$ should be much slower than the $O_2$ evolution rate over Pt−$WO_3$. Therefore, additional irradiation from illuminator B can be expected to increase the relative photon absorption by $BaTaO_2N$ and thereby lead to an enhancement of the $H_2$ and $O_2$ evolution rates. Figure 8 plots the ratio of the total evolution rate ($r_{A+B}$) to that due to illuminator A alone ($r_A$) as a function of the cutoff wavelength of illuminator B. Data for Pt−$CaTaO_2N$ (absorption edge, 520 nm) combined with Pt−$WO_3$ is also shown for comparison. In the case of $BaTaO_2N$, a ratio of 1.36 was

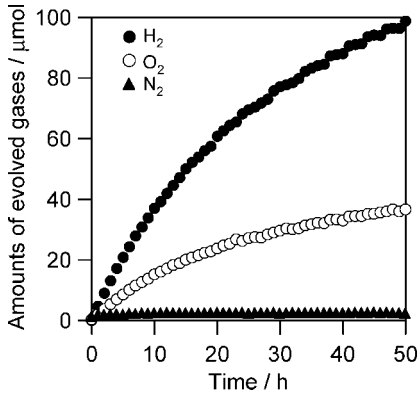


**Figure 9.** Time courses of $H_2$ and $O_2$ evolution over a mixture of Pt−$BaTaO_2N$ (30 mg) and Pt−$WO_3$ (30 mg) in aqueous 5 mM NaI solution under visible light ($\lambda > 420$ nm).

obtained with the 500 nm cutoff wavelength for illuminator B, indicating that the $H_2$ evolution rate over Pt−$BaTaO_2N$ is enhanced by increasing the total flux of incident photons, leading to an increase in the overall reaction rate (data not shown). The degree of enhancement of $H_2$ evolution ($r_{A+B}/r_A$) decreased with increasing cutoff wavelength, eventually reaching unity, indicating no enhancement under additional irradiation at wavelengths longer than 660 nm. These results demonstrate that the absorption of $BaTaO_2N$ at wavelengths up to 660 nm contributes to $H_2$ evolution in the overall water-splitting reaction. For $CaTaO_2N$, the enhancement of $H_2$ evolution was observed at wavelength below 520 nm, consistent with the absorption edge determined for $CaTaO_2N$.

**Stability of $BaTaO_2N$.** The stability of Pt−$BaTaO_2N$ in this system was evaluated by performing the water-splitting reaction under visible irradiation ($\lambda > 420$ nm) for a period of 50 h using small amounts of Pt−$BaTaO_2N$ (30 mg) and Pt−$WO_3$ (30 mg) in aqueous NaI solution (5 mM) (Figure 9). As shown in Figure 9, the total amount of evolved $H_2$ reached ca. 95 $\mu$mol, exceeding the molar amount of $BaTaO_2N$ photocatalyst (82.4 $\mu$mol). Although a small amount of $N_2$ was detected ($\sim$2.5 $\mu$mol for 10 h) in an initial period, the increase in $N_2$ amount was not observed after 10 h of irradiation. Therefore, the $N_2$ gas was certainly derived from residual $N_2$ in the solution before reaction, or possibly from partial self-oxidation of $BaTaO_2N$ photocatalyst. No structural change in the photocatalysts could be detected by XRD analysis after the reaction. The catalytic reaction was thus confirmed to proceed. However, the rate of gas evolution gradually decreased over time, and the ratio of evolved $H_2$ to $O_2$ deviated from stoichiometry with prolonged photoreaction. An accumulation of $I_3^-$ species was confirmed in the solution after the extended reaction, suggesting that the $I_3^-$ species are responsible for the observed deactivation. It appears that $I_3^-$ is not as efficient an electron acceptor as $IO_3^-$ for oxide semiconductors, attributable to the poorer adsorption characteristics of $I_3^-$.[23] It is therefore speculated that photoexcited electrons on Pt−$WO_3$ are unable to reduce $I_3^-$ effectively, resulting in suppressed $O_2$ evolution and the gradual accumulation of $I_3^-$ in the solution as the reaction proceeds. The origin of $I_3^-$ is considered to be the oxidation of $I^-$ by holes ($3I^- + 2h^+ \rightarrow I_3^-$) over Pt−$BaTaO_2N$ or Pt−$WO_3$. Distinguishing between these two sites for $I^-$ oxidation is difficult. Although such accumulation of $I_3^-$ can be solved by using alkaline solution with pH above 9 as reported previously,[23] we could not apply alkaline conditions in this system because $WO_3$ is unstable in alkaline media. Therefore, the development of a visible-light responsive photocatalyst with good stability in alkaline conditions is strongly desired to replace $WO_3$.

## Conclusion

Platinum-loaded $ATaO_2N$ (A = Ca, Sr, Ba) prepared by heating amorphous $A_2Ta_2O_7$ under $NH_3$ flow were found to exhibit photocatalytic activity for $H_2$ evolution from water under visible light in the presence of methanol or iodide ($I^-$) as an electron donor. Pt−$SrTaO_2N$ was found to be affected by self-oxidative decomposition, resulting in the release of $N_2$ in the presence of $I^-$. The combination of Pt−$BaTaO_2N$ or Pt−$CaTaO_2N$ and Pt−$WO_3$ was demonstrated to achieve overall water splitting under visible light in the presence of $IO_3^-/I^-$ as a shuttle redox mediator. Photoabsorption by $BaTaO_2N$ was confirmed to extend to wavelengths as long as 660 nm, representing the first example of an overall water-splitting system activated by light at wavelengths longer that than 600 nm. These results demonstrate the potential of a two-step water-splitting system for utilizing a broader band of the visible spectrum.

**Supporting Information Available:** Time courses of gas evolution over a mixture of Pt−$WO_3$ and Pt−$ATaO_2N$ (A = Ca or Sr) under visible light ($\lambda > 420$ nm) in the presence of 5 mM NaI (Pt(0.3 wt %)−$ATaO_2N$, 0.1 g, Pt(0.5 wt %)−$WO_3$, 0.1 g). Preparation temperature dependence of photocatalytic activity of a combination of Pt−$WO_3$ and Pt−$ATaO_2N$ (A = Ca or Sr). This material is available free of charge via the Internet at http://pubs.acs.org.

CM803145N